


# Invariant points amidst gauge sensitivity in cylindrical and toroidal lattices

Caelan Brooks<sup>1,2</sup> and Kunal K. Das<sup>2,3</sup>

<sup>1</sup>*Department of Physics, Harvard University, Cambridge, Massachusetts 02138, USA*

<sup>2</sup>*Department of Physical Sciences, Kutztown University of Pennsylvania, Kutztown, Pennsylvania 19530, USA*

<sup>3</sup>*Department of Physics and Astronomy, Stony Brook University, New York 11794-3800, USA*

 (Received 12 September 2022; revised 6 February 2024; accepted 8 February 2024; published 5 March 2024)

We examine the spectrum for lattices with cylindrical and toroidal topology subject to Abelian gauge potentials. Gauges that are equivalent in planar lattices with trivial topology develop differences due to the periodic boundary conditions. But some residual gauge equivalency, evident in the spectrum, is found to remain under specific conditions. This is associated with the gauge structure being commensurate with the lattice periodicity, and the behavior of the associated field along the symmetry axes. The interplay of the gauge choice and the periodic boundary conditions leads to a class of persistent degeneracies that are found to be robust against vast changes in system parameters and even under change of topology from cylinder to torus.

DOI: [10.1103/PhysRevB.109.115404](https://doi.org/10.1103/PhysRevB.109.115404)

## I. INTRODUCTION

The quantum mechanical description of electrons in a two dimensional (2D) lattice potential subject to a magnetic field has been a seminal model in physics leading to an appreciation of topological effects in many body quantum systems [1]. The most recognizable feature of this system is the fractal spectrum known as the Hofstadter butterfly [2]. The spectrum as well as the typical considerations assume an infinite lattice [3] with flexible choice of gauge [4]. However, cylindrical and toroidal topologies were famously invoked in two seminal models, Laughlin [5] and TKNN [6], to explain the quantum Hall effect [7]. With advances in optical lattices and synthetic gauge fields [8,9], creation of these configurations has gained renewed interest [10–15]. An interesting alternative route has utilized synthetic dimensions to implement such configurations wherein the periodic boundary condition is implemented by cyclic coupling of internal states [16–19]. These new developments have led to experimental realization of established theoretical models that have been challenging to realize previously [20], as well as the discovery of new phenomena [21,22].

For finite systems with periodic boundary conditions the typical gauges used in planar lattices with trivial topology lose their characteristic equivalency. This directly impacts the physical properties of the system, and specifically the differences become clearly evident in the spectrum. Yet, under certain conditions some of those gauges continue to present identical spectral features even in the presence of the periodic boundary conditions. In some cases, slightly shifting the gauge can act like a perturbation about those regimes of agreement. Significantly, we find that certain features remain remarkably robust against drastic variations of system parameters for certain gauge choices. They can remain invariant even on changing the topology of the system from a cylinder to a torus. The purpose of this paper is to identify and analyze those invariant features. We will present them in the context of a cylinder first then show how they also apply to a torus.

In Sec. II, we present our physical model and describe how we analyze the spectra for different configurations. Section III describes the interplay of the gauge choices and the boundary conditions. The essential invariant feature of persistent degeneracies is described in Sec. IV, followed by a comparison of the impact of different gauge choices in a cylindrical lattice in Sec. V. We then describe in Sec. VI how these features translate to a toroidal lattice configuration. We summarize our main findings in Sec. VII.

## II. PHYSICAL MODEL

Consider a quantum mechanical system of particles in a finite 2D lattice potential, its  $x$  and  $y$  orientations indexed by  $m \in \{1, \dots, M\}$  and  $n \in \{1, \dots, N\}$  respectively, and described by the Hamiltonian,  $H(n, m)$ :

$$\sum_{m,n} [J_x e^{-i2\pi\alpha f(n)} \psi_{n,m+1} + J_y e^{-i2\pi\alpha g(m)} \psi_{n+1,m} + J_x e^{i2\pi\alpha f(n)} \psi_{n,m-1} + J_y e^{i2\pi\alpha g(m)} \psi_{n-1,m}], \quad (1)$$

where we allow for different nearest neighbor hopping strengths  $J_x$  and  $J_y$  in the two relevant directions, with lattice spacings  $a_x$  and  $a_y$ . The parameter  $\alpha = qBa_x a_y / h$  is due to a magnetic field along  $z$ . The factors  $f(n)$  and  $g(m)$  are associated with the vector potential and set the gauge: For example, Landau  $x$  and  $y$  gauges would have  $f(n) = -n$ ,  $g(m) = 0$  and  $f(n) = 0$ ,  $g(m) = m$ , and the symmetric gauge  $f(n) = \mp \frac{1}{2}n$ ,  $g(m) = \pm \frac{1}{2}m$ , corresponding to continuum vector potentials  $\vec{A} = (-By, 0, 0)$ ,  $\vec{A} = (0, Bx, 0)$ , and  $\vec{A} = (\mp \frac{1}{2}By, \pm \frac{1}{2}Bx, 0)$ . In general, the vector potential can be parametrized as

$$\vec{A} = \left( \mp \frac{r}{s} By, \pm \frac{s-r}{s} Bx, 0 \right) \\ r \in \{0, 1, 2, \dots\} \quad s \in \{1, 2, \dots\} \quad (2)$$

so that  $f(n) = \mp \frac{r}{s}n$  and  $g(m) = \pm \frac{s-r}{s}m$ . The Landau gauges, referred to henceforth as  $x$  and  $y$  gauges, are limiting cases

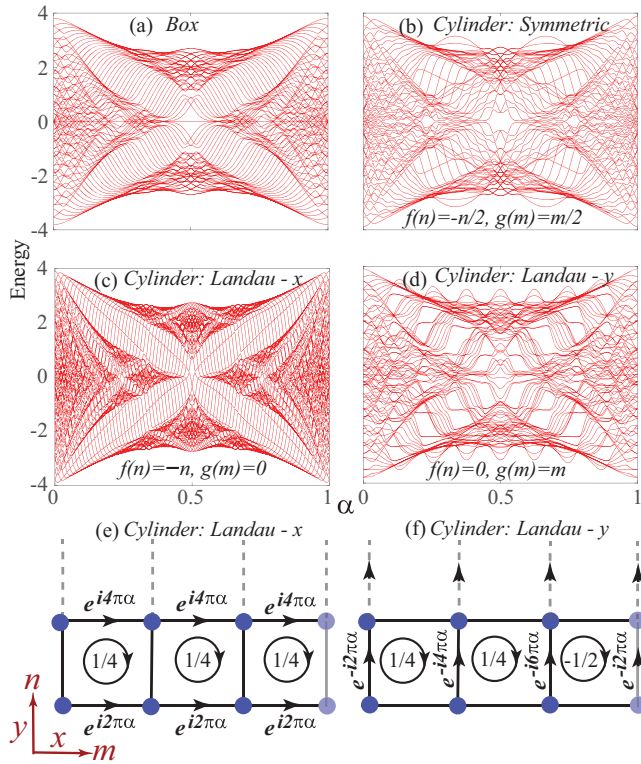


FIG. 1. The effect of the boundary condition and choice of gauge is illustrated for a  $9 \times 9$  lattice: (a) for hard wall boundary in both directions and (b), (c), (d) with periodic boundary along the  $x$  orientation but differing in the gauge used as indicated. (e), (f) The flux per plaquette for  $\alpha = 1/4$  is shown schematically for a cylindrical lattice with  $M = 3$  sites in the periodic direction, the rightmost sites being identical to the leftmost ones; the Landau  $x$  gauge maintains uniform flux, while the Landau  $y$  gauge is nonuniform.

with  $r = s$  and  $r = 0$ , respectively. All other gauges with other values of  $r, s$ , we will call split gauges.

Cylindrical topology can be introduced by imposing periodic boundary conditions along either orientation such that  $N + 1 \equiv 1$  or  $M + 1 \equiv 1$ ; without loss of generality we pick the latter as shown in Fig. 1. Insisting on both creates a torus topology. For cylindrical topology, the periodic boundary condition breaks the equivalency of these different gauges, as evident in the spectrum in Fig. 1, where we compare plots of  $9 \times 9$  lattices as a function of  $\alpha$ : One presents box boundary conditions and the other three have a cylindrical configuration each with a different gauge. Although the well-known butterfly shape is present in all, they are very distinct. The box boundary spectrum is insensitive to the choice of gauge, while the spectrum in the cylindrical configuration varies significantly with the gauge.

The energy spectra is computed by diagonalizing the Hamiltonian in Eq. (1) in the MATLAB computational software [23]. We map the 2D Hamiltonian to a 1D ordered array, and adjust the boundary conditions by setting array elements corresponding to the coupling of sites at opposite edges either to zero for box boundary conditions or equal to the relevant coupling coefficients for a periodic boundary condition. The

gauge choices are made by specifying the functions  $f(n)$  and  $g(m)$ .

### III. INTERPLAY OF GAUGE AND BOUNDARY CONDITIONS

Contrasting the two Landau gauges highlights some of the key impacts of the gauge choice on observables when we introduce periodic boundary conditions. In the  $x$  gauge, the phase is collected along the periodic boundary, resulting in a net flux along the symmetry axis of the cylinder; this is clearly not possible with the  $y$  gauge. Both gauges can however produce a radial field tied to the net phase collected in a circuit about each plaquette. This is evident even in the continuum expressions [4],

$$\vec{B}_{x\text{-gauge}} = -B\hat{\rho} + \frac{By}{R}\hat{y} \quad \vec{B}_{y\text{-gauge}} = -B\hat{\rho}, \quad (3)$$

up to a sign defined by the charge, with  $R$  being the radius of the cylinder. In our choice of coordinates, the symmetry axis is along the  $y$  coordinate. When we consider the discrete lattice Hamiltonian, the differences between the  $x$  and  $y$  gauges become more prominent, as contrasted in Figs. 1(e) and 1(f): For the  $x$  gauge, the net flux through each plaquette is identical for any value of  $\alpha$ . However, for the  $y$  gauge, that is generally not the case as shown in Fig. 1(f) for  $\alpha = 1/4$ , and even the direction of the flux can change.

It is also clear that for the  $x$  gauge there is a net nonzero radial flux if we sum over all the plaquettes azimuthally since the flux has the same orientation in all of them. But, for the  $y$  gauge the net radial flux vanishes on summing over all the plaquettes along the azimuth. If we consider a transverse cross-sectional volume of the cylinder comprising of any number of its constituent coupled rings, the integrated net flux vanishes for both gauges; for the  $x$  gauge the axial contribution cancels out the radial contribution. This is as one would expect in the absence of singularities such as magnetic monopoles. It is interesting to note, net nonvanishing radial flux has been demonstrated with synthetic gauge fields [16,22].

In the discrete lattice Hamiltonian, a discontinuity is present in the radial flux for the  $y$  gauge, but never present in the  $x$  gauge, as contrasted in Figs. 1(e) and 1(f). This discontinuity is associated with the flux reversal that creates the vanishing of the net radial flux in this gauge. The discontinuity is interesting because, due to the cylindrical symmetry of the system, it cannot be predicted *a priori* where it would manifest, somewhat analogous to spontaneously broken symmetry.

While the flux remains the same in each plaquette, a different kind of discontinuity can arise in the  $x$  gauge, in the phase accumulated in a full azimuthal circuit. For example, in Fig. 1(e), phase of  $1.5\pi$  is accumulated in a circuit of the bottom ring for  $\alpha = 1/4$ . The requirement for the quantum state to be single valued would not be met for a stationary state unless the net phase accumulated in each circuit is a multiple of  $2\pi$ . Those would correspond to the allowed states for the system at rest. Configurations where that phase condition is not met can correspond to circulating states where the rotation rate will contribute the additional phase needed to meet the phase condition [24].

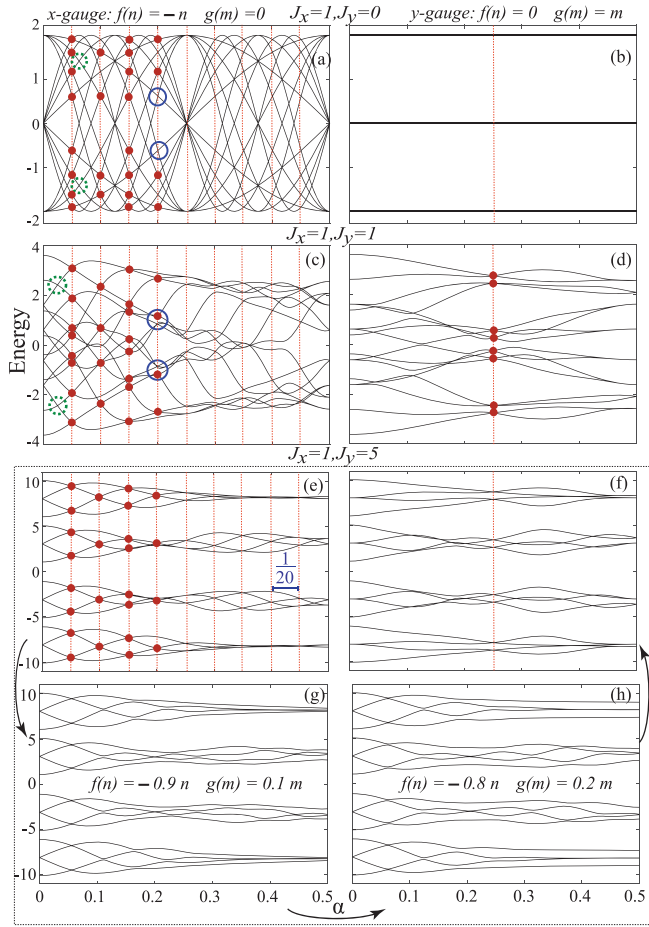


FIG. 2. Spectra for a  $4 \times 4$  cylindrical lattice: (a)–(f) Vary coupling  $J_y$  at fixed  $J_x$  for Landau gauge along periodic ( $x$ ) and open ( $y$ ) directions on left and right columns, respectively. Examples of slideby of spectral lines are marked by dotted line circles, avoided crossings by solid line circles, and persistent degeneracies by red dots [shown for left half only in (a), (c), (e), but leaving out the ones on the axis at  $\alpha = 0$ ]. Vertical dotted lines show the persistence of degeneracies at the same  $\alpha$  values. The panel sequence (e  $\rightarrow$  g  $\rightarrow$  h  $\rightarrow$  f) tracks gauge change at fixed  $J_x = 1$ ,  $J_y = 5$  from Landau  $x$  to Landau  $y$  by splitting the parameters  $f(n)$ ,  $g(m)$ ; persistent degeneracies disappear, with reappearance only at spectral equivalent point  $\alpha = 0.25$  for the  $y$  gauge.

#### IV. PERSISTENT DEGENERACIES

Despite its complexity, several features stand out in the energy spectrum, best illustrated in the context of the  $x$  gauge. In the limit  $J_y/J_x \rightarrow 0$ , shown in Fig. 2(a), we have a system of decoupled rings. Plotted as a function of  $\alpha$ , there are  $N \times M$  distinct spectral curves defined by the energies

$$E_{n,m} = 2J_x \cos\left(\frac{2\pi m}{M} - 2\pi\alpha n\right). \quad (4)$$

Each of the  $n \in \{1, 2, \dots, N\}$  rings contributes a set of  $M$  sinusoidal spectral curves of set period  $1/n$  but phase shifted by  $2\pi m/M$ ,  $m \in \{1, 2, \dots, M\}$ . The multitude of intersections that mark degeneracies at this limit fall into a few distinct categories which determine the behavior as the inter ring coupling  $J_y$  is turned on.

The most trivial intersections are between spectral lines representing different states (different  $m$ ) from the same ring (same  $n$ ). They slide by each other as  $J_y$  is increased until the lines separate and form parts of different bands. These intersections occur between spectral curves of the same period but different phase. Intersections between curves representing the corresponding states (same  $m$ ) on different rings (different  $n$ ), for example, ground state of each ring, lead to avoided crossings which mark a mixing of the states. When the coupling  $J_y$  between rings is raised sufficiently, these intersections split and widen, just as band gaps open up in multiple-well systems. Stronger coupling is needed to blend states on rings which are further away from each other.

The most interesting feature is the case of intersections that occur between spectral lines corresponding to different states (different  $m$ ) from different rings (different  $n$ ). They persist at exactly the same value of  $\alpha$  regardless of the value of the coupling ratio  $J_y/J_x$ . This is remarkable because the shape of the entire spectrum changes dramatically with changing  $J_y/J_x$  as seen in Fig. 2. In the case of an odd number of rings  $N$ , these intersections can also occur between different states from the same ring, but only for the central ring. Figure 2 indicates that persistent degeneracies appear in both Landau gauges, but with different origins as will be shown.

We find that persistent degeneracies occur at  $\alpha$  values which meet the condition

$$\alpha M(N+1) = k, \quad (5)$$

with integer  $k$ , in the case of a closed boundary condition in the  $x$  direction. Thus, in Figs. 2(a), 2(c), and 2(e), with  $(N, M) = (4, 4)$ , the vertical dotted lines are at  $\alpha = k/(4 \times 5) = 0.05 \times k$  with  $k \in \{0, 1, 2, \dots\}$ . While the factor  $M$  has a clear interpretation tied to the phase acquired in as many hops about a ring in a full circuit, the dependence on  $N+1$  instead of  $N$  is initially puzzling. The explanation resides in the fact that persistent degeneracies occur between spectral curves originating from rings which are complementary, ring  $1, 2, \dots$ , with ring  $N, N-1, \dots$ , respectively. This is illustrated in Fig. 3. In the case of odd value  $N$ , the center ring forms its own complement.

This is a curious relation, seeming to require phase acquired cooperatively between complementary pairs of rings to add up to a multiple of  $2\pi$ . It is intriguing that the complementary pairing varies with the number of rings in the cylinder, as seen in Eq. (5), but what is fixed is the ordering of the paired rings relative to the two edges. Even though such pairing and identification makes some sense when the rings are isolated, the degeneracies endure when the system has no resemblance to individual rings, and spectral expressions become too complex to have tractable analytic descriptions.

#### V. GAUGE COMPARISON FOR A CYLINDER

##### A. Gauge as perturbation

The  $x$  gauge plays a special role, as can be seen in the sequence of panels Figs. 2(e)  $\rightarrow$  2(g)  $\rightarrow$  2(h)  $\rightarrow$  2(f), where the gauge is varied from  $x$  to  $y$  as  $(f(1), g(1)) = (-1, 0) \rightarrow (-0.9, 0.1) \rightarrow (-0.8, 0.2) \rightarrow (0, 1)$  for fixed coupling  $J_x = 1$ ,  $J_y = 5$ . We find that gaps open up in all the persistent intersections as we perturb farther away from the  $x$  gauge,



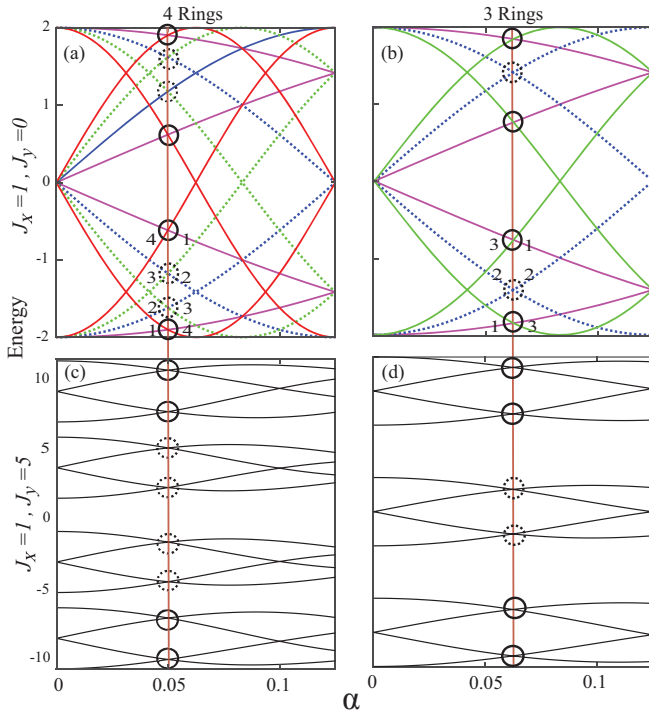


FIG. 3. In the Landau  $x$  gauge, persistent degeneracies occur between spectral curves that arise from complementary rings in a cylindrical lattice: (a), (c) In a  $4 \times 4$  lattice with an even number of rings, between rings 1,4 and 2,3; (b), (d) in a  $3 \times 4$  lattice with an odd number of rings they also occur between lines from the self-complementary center ring.

with the gauge component in the  $y$  orientation acting very much like a perturbation. In the pure  $y$  gauge itself, some persistent degeneracies remain as seen in Fig. 2, however they are substantially fewer and occur only at points of equivalency with the  $x$  gauge, discussed next. The perturbation of the persistent degeneracies at split gauges can be viewed as a failure to complete multiples of  $2\pi$  in a circuit, as the  $y$  gauge component “pulls away” phase accumulation from the  $x$  gauge component. As the split gauges defined in Eq. (2) skew more toward the  $y$  gauge, and  $|f(1)/g(1)|$  gets progressively smaller, the gaps widen at those degeneracy points.

### B. Spectral equivalent points

While the closed topology generally makes the system gauge sensitive, certain conditions allow a form of gauge equivalency to be restored. If the lattice is wrapped into a cylinder of  $M$  sites in the periodic direction, then if  $\alpha M|f(1)| = j$  with  $j = 1, 2, 3, \dots$ , both the Landau  $x$  and  $y$  gauges will have matching spectra for any ratio  $J_y/J_x$ . This condition assures that in an azimuthal circuit, the phase accumulated is a multiple of  $2\pi$ , removing the discontinuity in the  $x$  gauge mentioned in Sec. III. This is analogous to the Aharonov-Bohm condition for flux quantization [25].

The  $x$  and the  $y$  gauges continue to present distinct flux patterns, even at these points, with the former comprising of both radial and axial components while the latter only presents radial components. However, their spectral values

are identical. Comparing with the case of the box boundary condition provides an explanation, where the spectra for the two gauges are identical for any value of  $\alpha$ . This is because in the limit when either one of  $J_x$  or  $J_y$  vanishes, reducing such a system to a set of isolated 1D lattice strips, the spectrum has no dependence on  $\alpha$ . For box boundary conditions, for the gauge to have an impact on the spectrum, there has to be coupling in both  $x$  and  $y$  directions, and therefore is a consequence of the freedom of 2D motion. In a cylinder, on the other hand, when gauge factors appear in the hopping terms along the periodic direction, then even for an isolated 1D ring the spectrum presents nontrivial dependence on  $\alpha$  as can be seen from Eq. (4). But when the condition above is met,  $\alpha n = j/M$  [assuming  $f(n) = -n$ ], the terms in the argument of the cosine function in Eq. (4) become effectively the same, since the gauge periodicity is commensurate with the lattice period. Then, in a sense, the effect of the gauge “vanishes” for an isolated ring, as for a 1D strip. Thus, at those points, only the effects arising from the 2D coupling of the lattice sites remain, and the spectrum becomes equivalent for the two gauges, just as for a lattice with no periodic boundary conditions.

The spectral equivalence condition can be generalized for any pair of split gauges  $(f_1, g_1) \equiv (r_1, s_1)$  and  $(f_2, g_2) \equiv (r_2, s_2)$  which would occur, provided

$$\alpha M(|f_1(1)| - |f_2(1)|) = \alpha M \left( \frac{r_1}{s_1} - \frac{r_2}{s_2} \right) = k, \quad (6)$$

assuming closed boundary in the  $x$  orientation, and integer  $k$ . The difference between the phase collected around each ring under the influence of the two different gauges will be a multiple of  $2\pi$ . This provides a criterion for when a split gauge will match one of the Landau gauges. We can illustrate this by introducing an additional constant phase factor along the closed orientation,  $J_x \rightarrow J_x e^{i\varphi}$  marking an extra axial field such as assumed in the well-known Laughlin model for the quantum Hall effect [5]. In Fig. 4 we plot the spectra for two different gauges:  $x$  gauge  $(r_1, s_1) = (1, 1)$  and  $(r_2, s_2) = (4, 7)$  as a function of  $\varphi$  on a cylinder with the number of rings and sites  $(N, M) = (4, 4)$ . In panels (a) and (b), where  $\alpha = 2/3$ , the spectra are different, since the condition in Eq. (6) is not satisfied, but panel (c), for  $\alpha = 7/12$ , shows a spectrum identical for both gauges since that condition is met. That equivalence holds for arbitrary  $J_y/J_x$  even though the spectrum itself changes and, when plotted versus  $\alpha$ , is marked by both gauges always having the same eigenvalues at that point. When a split gauge matches the  $y$  gauge, the phase accumulated in an azimuthal circuit is necessarily a multiple of  $2\pi$ .

## VI. TORUS

We now consider if and how the features discussed above manifest in a toroidal lattice. Since a torus has periodic boundary conditions in both  $x$  and  $y$  orientations, there can be two axial fields, one along each symmetry axis. For two different gauges to match, the condition in Eq. (6) has to be generalized to be satisfied in both orientations, giving us the two

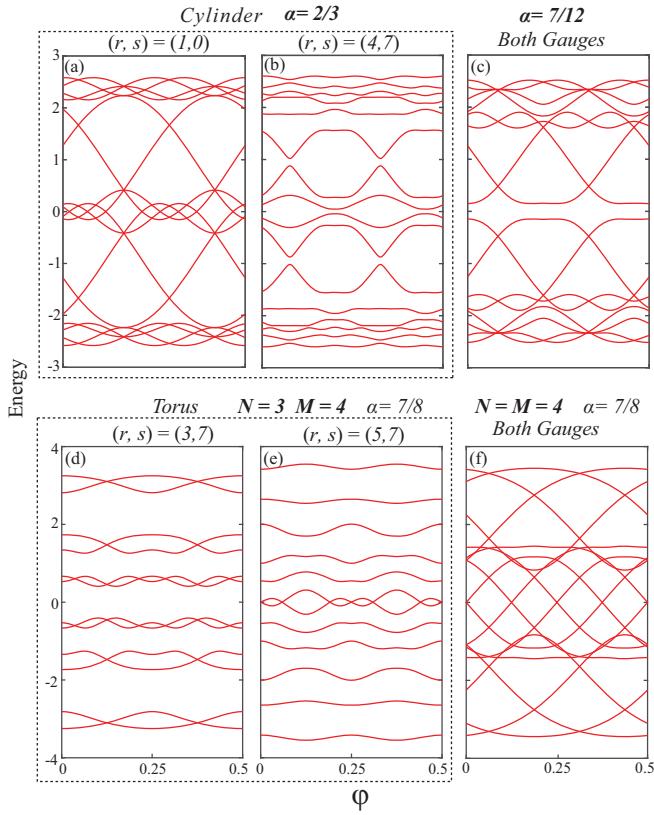


FIG. 4. (a), (b) The spectrum is plotted as a function of an additional phase  $\varphi$  in the hopping coupling  $J_x e^{i\varphi}$  along a direction with periodic boundary condition, which can represent an extra axial field. For a cylindrical lattice, the spectra differs for two gauges [labeled by values of  $(r, s)$ ] for arbitrary values of the gauge parameter  $\alpha$ , for example for  $\alpha = 2/3$  in panels (a) and (b), but for certain values, such as  $\alpha = 7/12$ , that satisfy Eq. (6) the two gauges present the same spectrum shown in panel (c). For a torus along with  $\alpha$ , the symmetry of the lattice is a relevant factor: (d), (e) for  $\alpha = 7/8$  the two gauges considered present different spectra when the number of sites along two axes differ  $N \neq M$ , but present the same spectrum shown in panel (f) when  $N = M$ .

conditions (with integer  $k$  and  $k'$ ),

$$\begin{aligned} \alpha M(|f_1(1)| - |f_2(1)|) &= k \\ \alpha N(|g_1(1)| - |g_2(1)|) &= k', \end{aligned} \quad (7)$$

which requires axial fields to match along both orientations up to multiples of  $2\pi$ . The second condition can also be written as  $\alpha N[|f_1(1)| - |f_2(1)|] = -k'$ , since  $g(1) - f(1) = 1$ . So in the case of a symmetric torus when  $M = N$ , one condition guarantees the other. This is illustrated in Figs. 4(d) and 4(e), where two gauges  $(r_1, s_1) = (3, 7)$  and  $(r_2, s_2) = (5, 7)$  yield different spectra for  $\alpha = 7/8$  when  $(N, M) = (3, 4)$ , since the second condition above is not satisfied. But, Fig. 4(f) displays identical spectra presented by both of these gauges for the same value of the parameter  $\alpha$  when the lattice becomes symmetric with the same number of sites along both axes,  $N = M = 4$ . Even for asymmetric tori,  $N \neq M$ , the spectral equivalency between the gauges will occur for those values of  $\alpha$  which satisfy both conditions. Clearly with two conditions

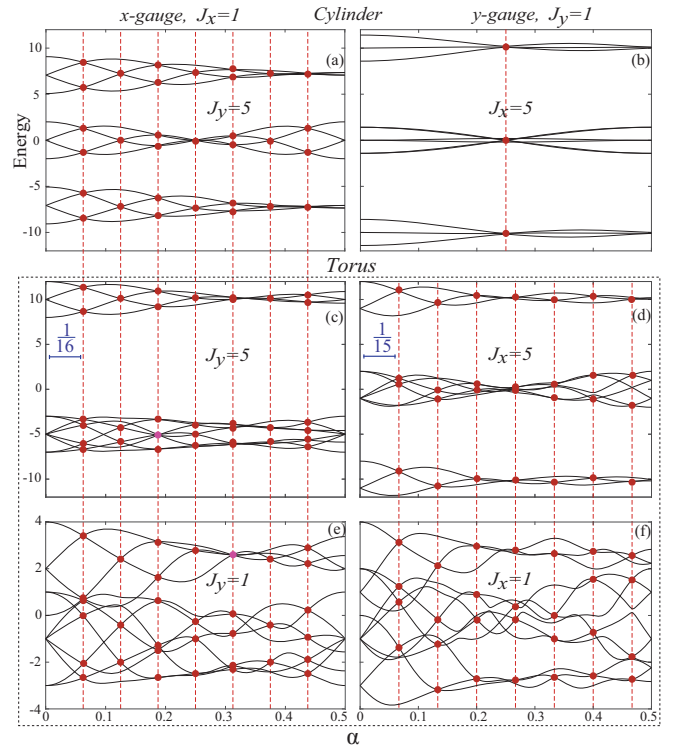


FIG. 5. Persistent degeneracies appear in the spectrum of a torus  $(N, M) = (3, 4)$  marked by red dots with dashed lines showing the invariant  $\alpha$  as the coupling ratio varies (the ones on the axes at  $\alpha = 0, 0.5$  are not marked). Left and right columns present  $x$  and  $y$  gauges, respectively. In transition from (a) a cylinder with  $x$  gauge (all gauge in periodic direction) to (c), (e) torus, the spectrum changes but the  $\alpha$  values for the degeneracies are invariant. (b) A cylinder with  $y$  gauge (all gauge in open direction) only has such degeneracy where it matches the  $x$  gauge, yet numerous new persistent degeneracies emerge in transitioning to a torus (d), (e).

instead of one, such equivalency is more restricted for a torus than for a cylinder.

We find that persistent degeneracies also occur in the torus at  $\alpha$  values which meet the condition in Eq. (5) that we presented in the context of cylindrical lattices. But now, with periodic boundary conditions in both directions, that expression has to be interpreted to mean that the gauge factor on the hopping potential appears only along the direction indexed by  $M$  which, without loss of generality, we assume to be the  $x$  gauge. If we switch to a  $y$  gauge, we simply switch  $N \leftrightarrow M$  in that expression. Specifically, this implies that if we have a cylinder with  $x$  gauge, the  $\alpha$  values where the persistent degeneracies occur will not change if we convert to a torus, although the general spectrum changes. This is shown in Figs. 5(a), 5(c), and 5(e) with  $(N, M) = (3, 4)$ ; the vertical lines marking the persistent degeneracies are shown at  $\alpha = k/(N \times M) = k/16$ , with  $k \in \{0, 1, 2, \dots\}$  for both the cylinder and the torus. For the same cylinder, with  $y$  gauge, persistent degeneracies only occur at points of equivalency with  $x$  gauge which satisfy Eq. (6), such as at  $\alpha = 1/4$  as seen in Fig. 5(b). However, in the torus created by closing that cylinder, numerous persistent degeneracies are seen to occur for  $\alpha = k/(3 \times 5)$  with  $k \in \{0, 1, 2, \dots\}$  in Figs. 5(d) and

5(f) corresponding to switching  $N \leftrightarrow M$  in Eq. (5). Notably, the degeneracy point in the  $y$ -gauge cylinder does not correspond to any of those persistent degeneracies that appear in the torus, underscoring the crucial role of boundary conditions.

For a torus, Figs. 5(c)–5(f) establish that persistent intersections occur for both Landau gauges. Hence, split gauges can have persistent degeneracies when there is spectral equivalency with either of the two Landau gauges in the sense of Eq. (6), if that equivalency occurs at a persistent degeneracy for the latter. The same applies to a cylinder, but the equivalency has to be with the  $x$  gauge.

## VII. CONCLUSIONS

We have shown that typical gauge equivalency assumed in open 2D lattices subject to a perpendicular magnetic field is clearly not applicable in finite systems with nontrivial topology. These gauges now correspond to fundamentally different fields and fluxes with distinct characteristics. Yet, certain residual equivalency, evident in the spectrum, remains between specific pairs of gauges under conditions that we identify. Despite that loss of equivalency among commonly used gauges, we found that the spectrum for such topologically nontrivial lattices can present persistent degeneracies that occur at the same specific values of the characteristic

parameter  $\alpha$ . They remain remarkably robust across the complete range of coupling ratios,  $J_y/J_x$  and even under change of topology from cylinder to torus under certain conditions. Such persistent degeneracies do not seem to be present in lattices with box boundary conditions along both axes. Even for cylindrical and toroidal lattices, they occur for particular choice of the gauge. This indicates that these features are characteristic of the interplay of gauge structure and the periodic boundary condition.

Small lattices as we consider here tend to highlight such features and suggest that, particularly in the context of topologically nontrivial lattices, interesting new phenomena can be explored that may be suppressed for large systems. In future work, we plan to examine the implications of these features on the stationary states of the system. These invariant points can offer a novel way to characterize and understand properties of such systems with nontrivial topologies. Systems with non-Abelian gauge fields may also provide interesting counterparts to our findings.

## ACKNOWLEDGMENTS

This work was supported by NSF under Grants No. PHY-2011767 and No. PHY-2309025. We thank A. Brattley for valuable discussions.

- 
- [1] D. J. Thouless, *Topological Quantum Numbers in Nonrelativistic Physics* (World Scientific, Singapore, 1998).
  - [2] D. R. Hofstadter, Energy levels and wave functions of Bloch electrons in rational and irrational magnetic fields, *Phys. Rev. B* **14**, 2239 (1976).
  - [3] P. G. Harper, Single band motion of conduction electrons in a uniform magnetic field, *Proc. Phys. Soc. A* **68**, 874 (1955).
  - [4] C. Cohen-Tannoudji, B. Diu, and F. Lalo e, *Quantum Mechanics* (Wiley, New York, NY, 1977).
  - [5] R. B. Laughlin, Quantized Hall conductivity in two dimensions, *Phys. Rev. B* **23**, 5632 (1981).
  - [6] D. J. Thouless, M. Kohmoto, M. P. Nightingale, and M. den Nijs, Quantized Hall conductance in a two-dimensional periodic potential, *Phys. Rev. Lett.* **49**, 405 (1982).
  - [7] M. Stone, *Quantum Hall Effect*, 1st ed. (World Scientific, 2001).
  - [8] N. Goldman, J. C. Budich, and P. Zoller, Topological quantum matter with ultracold gases in optical lattices, *Nat. Phys.* **12**, 639 (2016).
  - [9] N. Goldman, G. Juzeli unas, P.  ohberg, and I. B. Spielman, Light-induced gauge fields for ultracold atoms, *Rep. Prog. Phys.* **77**, 126401 (2014).
  - [10] H. Kim, G. Zhu, J. V. Porto, and M. Hafezi, Optical lattice with torus topology, *Phys. Rev. Lett.* **121**, 133002 (2018).
  - [11] M.  acki, H. Pichler, A. Sterdyniak, A. Lyras, V. E. Lembessis, O. Al-Dossary, J. C. Budich, and P. Zoller, Quantum Hall physics with cold atoms in cylindrical optical lattices, *Phys. Rev. A* **93**, 013604 (2016).
  - [12] J. C. Budich, A. Elben, M. Lacki, A. Sterdyniak, M. A. Baranov, and P. Zoller, Coupled atomic wires in a synthetic magnetic field, *Phys. Rev. A* **95**, 043632 (2017).
  - [13] P. Rosson, M. Lubasch, M. Kiffner, and D. Jaksch, Bosonic fractional quantum Hall states on a finite cylinder, *Phys. Rev. A* **99**, 033603 (2019).
  - [14] T.-L. Ho and B. Huang, Spinor condensates on a cylindrical surface in synthetic gauge fields, *Phys. Rev. Lett.* **115**, 155304 (2015).
  - [15] E. Lustig, M.-I. Cohen, R. Bekenstein, G. Harari, M. A. Bandres, and M. Segev, Curved-space topological phases in photonic lattices, *Phys. Rev. A* **96**, 041804(R) (2017).
  - [16] R. Zhang, Y. Yan, and Q. Zhou, Localization on a synthetic Hall cylinder, *Phys. Rev. Lett.* **126**, 193001 (2021).
  - [17] Y. Yan, S.-L. Zhang, S. Choudhury, and Q. Zhou, Emergent periodic and quasiperiodic lattices on surfaces of synthetic Hall tori and synthetic Hall cylinders, *Phys. Rev. Lett.* **123**, 260405 (2019).
  - [18] Q.-Y. Liang, D. Trypogeorgos, A. Vald es-Curiel, J. Tao, M. Zhao, and I. B. Spielman, Coherence and decoherence in the Harper-Hofstadter model, *Phys. Rev. Res.* **3**, 023058 (2021).
  - [19] J. H. Han, D. Bae, and Y. Shin, Synthetic Hall ladder with tunable magnetic flux, *Phys. Rev. A* **105**, 043306 (2022).
  - [20] A. Fabre, J.-B. Bouhiron, T. Satoor, R. Lopes, and S. Nascimbene, Laughlin’s topological charge pump in an atomic Hall cylinder, *Phys. Rev. Lett.* **128**, 173202 (2022).
  - [21] J. H. Han, J. H. Kang, and Y. Shin, Band gap closing in a synthetic Hall tube of neutral fermions, *Phys. Rev. Lett.* **122**, 065303 (2019).
  - [22] C.-H. Li, Y. Yan, S.-W. Feng, S. Choudhury, D. B. Blasing, Q. Zhou, and Y. P. Chen, Bose-Einstein condensate on a synthetic topological Hall cylinder, *PRX Quantum* **3**, 010316 (2022).
  - [23] The MathWorks Inc., MATLAB version: 9.13.0 (R2022b) (2022).
  - [24] H. Huang and K. K. Das, Effects of a rotating periodic lattice on coherent quantum states in a ring topology: The case of positive nonlinearity, *Phys. Rev. A* **104**, 053320 (2021).
  - [25] Y. Aharonov and D. Bohm, Significance of electromagnetic potentials in the quantum theory, *Phys. Rev.* **115**, 485 (1959).